The involvement of sodium in the function of the human amino acid transporter ASCT2

Tiziano Mazza[1], Mariafrancesca Scalise[1], Gilda Pappacoda[1], Lorena Pochini[1] and Cesare Indiveri[1,2] (iD)

1 Department DiBEST (Biologia, Ecologia, Scienze Della Terra) Unit of Biochemistry and Molecular Biotechnology, University of Calabria, Arcavacata di Rende, Italy
2 CNR Institute of Biomembranes, Bioenergetics and Molecular Biotechnology (IBIOM), Bari, Italy

Correspondence

C. Indiveri, Department DiBEST (Biologia, Ecologia e Scienze della Terra) University of Calabria Via P. Bucci cubo 4C, 87036 Arcavacata di Rende (CS) Italy
Tel: +39-0984-492939
E-mail: cesare.indiveri@unical.it

Tiziano Mazza and Mariafrancesca Scalise contributed equally to this work.

Alanine, serine, cysteine transporter 2 (ASCT2) is a membrane amino acid transporter with relevance to human physiology and pathology, such as cancer. Notwithstanding, the study on the ASCT2 transport cycle still has unknown aspects, such as the role of Na^+ in this process. We investigate this issue using recombinant hASCT2 reconstituted in proteoliposomes. Changes in the composition of purification buffers show the crucial role of Na^+ in ASCT2 functionality. The transport activity is abolished when Na^+ is absent or substituted by Li^+ or K^+ in purification buffers. By employing a Na^+ fluorometric probe, we measured an inwardly directed flux of Na^+ and, by combining fluorometric and radiometric assays, determined a $2Na^+ : 1Gln$ stoichiometry. Kinetics of Na^+ transport suggest that pH-sensitive residues are involved in Na^+ binding/transport. Our results clarify the role of Na^+ on human ASCT2 transporter activity.

The membrane transporter alanine, serine, cysteine transporter 2 (ASCT2; SLC1A5) belongs, together with ASCT1 (SLC1A4), to a small sub-group of proteins included in the SoLute Carriers 1 (SLC1) family and responsible for the traffic of neutral amino acids across plasma membranes. This sub-group is differentiated in terms of both sequence similarity and function from the other five members of the family that are high-affinity glutamate transporters, mainly responsible for the re-uptake of glutamate released in synapses [1,2]. Over the years, ASCT2 has attracted more attention than ASCT1 due to its involvement in human cancer metabolism, which was described at the beginning of the twenty-first century [3]. This remarkable interest can be deduced by the sizable number of papers published on ASCT2, that brought to an advanced functional and, more recently, structural knowledge of this transporter. Since the first isolation of the murine and human gene, the functional and kinetic characterization of ASCT2 has been performed in different experimental models, i.e. intact cells and proteoliposomes [4–8]. It has been clearly shown that the transport reaction catalysed by ASCT2 is an obligatory antiport of neutral amino acids, strictly Na^+-dependent. Over the years, functional and kinetic studies have been indistinctly conducted on murine or human ASCT2. Later on, it was highlighted that, despite the 79% sequence identity between the rat and human proteins, a low identity degree of only 14% exists in a stretch of roughly 30 amino acids. Similar

observations can be derived when comparing mouse and human ASCT2: even if the two proteins share 80% global identity, only 37% identity is present in the same 30 amino acid stretch. These are located in a region corresponding to an extracellular loop containing one of the two *N*-glycosylation sites of the hASCT2 (residues 200–229 of the hASCT2 sequence, Fig. S1) [9]. Another striking difference between the proteins of the three species is the number of cysteine residues in the sequence, i.e. 16 Cys in the rat protein, 14 in the mouse protein and eight Cys in the human protein. Owing to the role of Cys residues in proteins [10,11], this feature indicates a different sensitivity to redox regulation and/or response to thiol-reactive xenobiotics [12,13]. Therefore, the murine proteins cannot be unambiguously considered appropriate models for the hASCT2. This observation becomes even more important when considering that hASCT2 is a hot pharmacological target, due to the already mentioned overexpression in most human cancers [2,13,14]. As a consequence, in the last decade, all efforts have been focused on hASCT2. A milestone in these studies was the overexpression of the hASCT2 in *Pichia pastoris*, which allowed firstly to functionally characterize and to reveal some regulatory properties of the human protein [8], then, to approach its structure/function relationships [13] and, eventually to solve its structure [15]. Concerning the functional characterization of hASCT2, substrate specificity and kinetics have been defined with glutamine being the preferred substrate of hASCT2 with a sharp kinetic asymmetry. Indeed, Km values in the micromolar or the millimolar range have been measured for the substrates, on the external or internal side, respectively [8,16]. In a biological context, the most plausible transport reaction would be the exchange of glutamine from the external side with smaller amino acids, such as asparagine or serine from the internal side [17]. This reaction triggers a net uptake of 1–2 carbon atoms useful to fuel the TCA for energy production in either physiological or pathological conditions [17,18]. Furthermore, ASCT2 would participate in the balancing of amino acid pools in cells, functioning as a harmonizer [19,20]. Finally, an unusual transport of glutamate catalysed by hASCT2 has been very recently characterized [21]. This low-affinity Na$^+$ and H$^+$-dependent glutamate$_{ex}$/glutamine$_{in}$ antiport may be involved in the glutamate/glutamine cycle occurring in different body districts, including placenta/foetus or brain, as well as in some pathological conditions, such as cancer [21]. Despite the deep investigation of the hASCT2 transport cycle from the 'amino acid point of view', the actual role of Na$^+$ in the hASCT2 transport cycle is still uncertain. The

knowledge is limited to the need for this cation for the amino acid transport reaction from the external side [8] and an allosteric regulation from the internal side [16]. Again highlighting that the animal proteins are not suitable models for the human one, some differences in the involvement of Na$^+$ in the transport reaction exist among the hASCT2 and the mASCT2 [22] or the rASCT2 [23,24]. Interestingly, even if no bound sodium have been revealed in the recently solved 3D structures, three sodium binding sites in hASCT2 can be predicted based on the ASCT1 data (Figs S2 and S3); for this protein, indeed, the molecular determinants of three sodium binding sites have been previously described [2,15,25,26]. To the best of our knowledge, apart from the cited information, the actual involvement of Na$^+$ in the transport reaction or the protein functionality has never been addressed. Then, to shed light on this intriguing issue, we here present a study on the role of Na$^+$ on the hASCT2 produced in *P. pastoris* and on the involvement of the cation in the transport cycle, by setting up a fluorometric assay to directly measure the Na$^+$ flux.

Materials and methods

Materials

The *P. pastoris* wild type strain (X-33), the pPICZB vector, zeocin, Ni-NTA agarose resin, Sodium Green™ tetra(tetramethylammonium) salt were from Invitrogen (Life Technologies Italia, Monza, Italy); PD-10 columns were from GE Healthcare Italia (Napoli, Italy); L-[^{3}H]glutamine was from Perkin Elmer Italia (Milano, Italy); octaethylene glycol monododecyl ether (C$_{12}$E$_8$) was from TCI Europe (Zwijndrecht, Belgium); cholesterol, Amberlite XAD-4, egg yolk phospholipids (3-sn-phosphatidylcholine from egg yolk), Sephadex G-75, L-glutamine, and all the other reagents were from Sigma Aldrich Merck (Milano, Italy).

Recombinant production of hASCT2-6His

To produce the recombinant hASCT2-6His protein a previously pointed out approach was employed [8]. In brief: 10 µg of pPICZB-ASCT2-6His WT construct was linearized with PmeI, then the linearized plasmid was used to transform *P. pastoris* wild type strain X-33 by electroporation [27]. Before large-scale protein production, transformed *P. pastoris* cells were selected using YPDS plates containing 2000 µg·mL^{-1} zeocin; then, cells were inoculated in buffered glycerol-complex medium (BMGY) medium and grown at 30 °C under rotatory stirring [13]. Then, the BMGY medium was removed by centrifuging *P. pastoris* cells which were resuspended at final OD of 1 in 250 mL buffered complex methanol medium containing 0.5%

methanol. The cells were placed in a 2 L conical flask and grown in the same medium at 30 °C under rotatory stirring, for 3 days. Fresh methanol was added every 24 h to induce protein production. The *P. pastoris* membrane fraction was prepared starting from 30 to 40 g of cells resuspended in 300 mL of a buffer composed of 50 mM Tris HCl pH 7.4, 150 mM NaCl, 2 mM β-mercaptoethanol and 0.5 mM PMSF. The cell suspension was loaded in the chamber of a bead beater (BioSpec Product; BioSpec, Bartlesville, OK, USA) for disruption using glass beads (0.5 mm) for 5 min cycle reaching 90% of cell disruption. Then, the broken cell suspension was centrifuged in a JA10 rotor at 10 000 *g* for 30 min at 4 °C. The collected supernatant, containing membrane and cytosolic fractions, was subjected to centrifugation in a JA30.50 rotor at 45 000 *g* for 90 min at 4 °C. The resulting pellet containing membrane fraction was washed with a buffer composed of 5 mM Tris HCl pH 7.4, 2 mM EDTA, 2 mM EGTA and 4 M urea, followed by another centrifugation cycle as above described. The washed membrane fraction was resuspended in a buffer composed of 25 mM Tris HCl pH 7.4, 250 mM NaCl, 2 mM β-mercaptoethanol and 10% glycerol to reach a concentration of about 400 mg·mL^{-1}. The membranes were homogenized with a potter and 3 mL aliquots were stored at −80 °C before solubilization.

Solubilization and purification of hASCT2-6His

The purification of hASCT2-6His was performed starting from about 1.2 g of washed membranes (400 mg·mL^{-1}) that were solubilized in a buffer composed of 25 mM Tris HCl pH 7.4, 250 mM NaCl, 6 mM β-mercaptoethanol, 1 mM L-glutamine, 10% glycerol and 2% C$_{12}$E$_8$ (w/w). The solubilization was performed under rotatory stirring for 3 h at 4 °C followed by centrifugation at 18 000 *g* for 45 min. The supernatant was applied to 2 ml Ni-nitrilotriacetic acid (NTA) agarose resin pre-equilibrated with a buffer containing 20 mM Tris HCl pH 7.4, 300 mM NaCl, 10% glycerol, 6 mM β-mercaptoethanol, 0.03% C$_{12}$E$_8$, 1 mM L-glutamine and 50 mM imidazole and incubated overnight, with gentle agitation, at 4 °C. Then, the Ni-NTA resin was packed by gravity into a glass column and washed with 30 mL of the same buffer above described. Elution of protein was, then, performed using 10 mL of a buffer containing 20 mM Tris HCl pH 7.4, 300 mM NaCl, 10% glycerol, 6 mM β-mercaptoethanol, 0.03% C$_{12}$E$_8$, 1 mM L-glutamine and 500 mM imidazole. 2.5 mL of purified protein were pooled and desalted on a PD-10 column from which 3.5 mL were collected. The column was pre-equilibrated and eluted with a buffer composed of 20 mM Tris HCl pH 7.4, 100 mM NaCl (or different sodium concentration as specified in the figure legend), 10% glycerol, 6 mM β-mercaptoethanol, 0.03% C$_{12}$E$_8$ and 1 mM L-glutamine. To evaluate the presence of aggregates in the purified proteins, 1 mL of desalted protein was loaded onto a Sephacryl 16/60 S-200

HR for size exclusion chromatography (SEC). The column was equilibrated with a buffer composed of 20 mM Tris HCl pH 7.4, 300 mM NaCl (or without sodium), 10% glycerol, 6 mM β-mercaptoethanol, 0.003% C$_{12}$E$_8$ and 1 mM L-glutamine, and eluted with the same buffer using AKTA-Go system. Fractions of 2 mL were collected and analysed by SDS/PAGE.

Inclusion of cholesterol in liposome preparation

7.5 mg of cholesterol were added to 100 mg of egg yolk phospholipids and solubilized with 1mL of chloroform obtaining a completely clear solution. After short incubation under rotatory stirring (30 °C 5 min 1200 r.p.m. Model of the instrument: thermomixer C from Eppendorf Italia, Milano, Italy) the solution was dried with rotavapor at room temperature. The dried lipid film was resuspended in 1 mL water (10% final concentration) and unilamellar liposomes were formed by two sonication cycles of 1 min (1 pulse ON and 1 pulse OFF, 40 W) with a Vibracell VCX-130 sonifier as previously suggested [28].

Reconstitution of the hASCT2-6His into liposomes

The purified hASCT2 was reconstituted by detergent removal in a batch-wise procedure, in brief: mixed micelles of detergent, protein and phospholipids were incubated with 0.5 g Amberlite XAD-4 resin under rotatory stirring (1200 r.p.m.) at 23 °C for 40 min as previously described [29]. The composition of the reconstitution was: 50 μL of the purified hASCT2 (5 μg protein), 5 μL of EDTA 0.3 M, 220 μL of a mixture composed by 100 μL of 10% (w/v) egg yolk phospholipids with 7.5% cholesterol (w/w), in the form of sonicated liposomes and 120 μL of 10% C$_{12}$E$_8$, 10 mM L-glutamine (or other amino acids as specified in the figure legend), 20 mM Hepes Tris pH 7.0 (or different pH as specified in the figure legend) in a final volume of 700 μL. To increase the active-proteoliposome fraction without exceeding with Na⁺-containing buffer, the purified protein was desalted on a PD-10 column pre-equilibrated with the same buffer described in the above section, except that the NaCl concentration was 50 mM instead of 100 mM. The purified protein was then concentrated to 1 μg·μL^{-1} by using Amicon® (Merck Life Science, Milano, Italy) Ultra Centrifugal Filters cut-off 50K, then 25 μg of protein was used for the reconstitution mixture. All the operations were performed at room temperature.

Radiometric assay

To remove the external compounds, 600 μL of proteoliposomes was passed through a Sephadex G-75 column (0.7 cm diameter × 15 cm height) pre-equilibrated with a buffer composed of 20 mM Hepes Tris pH 7.0 and sucrose

to balance the internal osmolarity. Uptake experiments were started in a 100 µL proteoliposomes sample by adding 50 µM [^{3}H]-glutamine together with 50 mM Na-gluconate at 25 °C (Fig. 1A). The transport reaction was stopped at the indicated times using 10 µM HgCl$_2$. The control sample, i.e. blank, was prepared by adding the same inhibitor at time zero according to the inhibitor stop method [30]. At the end of the transport, 100 µL of proteoliposomes was passed through a Sephadex G-75 column (0.6 cm diameter × 8 cm height) buffered with 50 mM NaCl to separate the external from the internal taken up radioactivity. Then, proteoliposomes were eluted with 1 mL 50 mM NaCl and added with 3 mL of scintillation mixture, vortexed and counted. The experimental values were analysed by subtracting to each sample the respective blank; the initial rate of transport was measured by stopping the reaction after 15 min, i.e. within the initial linear range of radiolabelled substrate uptake into the proteoliposomes.

Spectrofluorometric assays

The intraliposomal sodium accumulation was monitored by measuring the fluorescence emission of Sodium Green™ (Invitrogen, Life Technologies Italia). After reconstitution, 600 µL of proteoliposomes was passed through a Sephadex G-75 column (0.7 cm diameter × 15 cm height) pre-equilibrated with 20 mM Hepes Tris pH 7.0. Uptake experiments were started in a 150 µL proteoliposome sample by adding 10 mM glutamine together with 50 mM Na-gluconate, at 25 °C (Fig. 1B). The transport reaction was stopped by 10 µM HgCl$_2$ at 60 min; to separate the external from the internally accumulated Na$^+$, samples were passed through a Sephadex G-75 column (0.6 cm diameter × 8 cm height) buffered with 20 mM Hepes Tris pH 7.0 and 20 mM sucrose; samples were then, eluted with 1 mL of the same buffer. The fluorometric assay was performed in 2 mL of eluted proteoliposome from the previous step added with a mixture of 50 nM Sodium Green™ and 0.25% C$_{12}$E$_8$ to destabilize proteoliposomes, allowing sodium green indicator (SGI) to interact with internally accumulated Na$^+$ (Fig. 1B). The measurements were performed in the fluorescence spectrometer (LS55) from Perkin Elmer under rotatory stirring. The fluorescence was measured following time drive acquisition protocol with λ excitation = 507 nm and λ emission = 532 nm (slit 5/5) according to manufacturer instructions of Sodium Green™. Calibration of the fluorescence changes vs released Na$^+$ has been performed by measuring the fluorescence of known amounts of Na$^+$-gluconate (from 0 to 2000 nmol in 2 mL) obtaining a linear correlation as previously performed [31]. The calibration line was used to calculate the nmoles of Na$^+$ taken up in hASCT2-harbouring proteoliposomes (Fig. 1C). A calibration was performed at the end of each experiment.

Stoichiometry evaluation

The stoichiometry of Na$^+$: Gln transport has been measured by parallel assays, both fluorometric and radiolabelled measurements, for Na$^+$ and Gln respectively, starting from the following assumption: the homologous 1 : 1 Gln antiport reaction in co-transport with Na$^+$, employed for the transport assay, does not generate any change of internal or external Gln concentration, being a cyclic process (Fig. 1A,B). Therefore, the nmoles of Gln virtually entered the internal space, in co-transport with Na$^+$, have been derived from the uptake of a tracer, i.e. [^{3}H]-glutamine (Fig. 1A). Differently from the cyclic process of the unlabelled Gln, the uptake of the tracer [^{3}H]-glutamine follows an equilibrative process described by a first-order rate equation: $Y = A(1 - e^{-kt})$, where Y and A are the nanomoles of substrates taken up at time t, and at infinite time, respectively (Table S1). From the equilibrative process, the transport rate can be evaluated (nmol·min^{-1}) as the product of the first-order rate constant of the antiport reaction k and A [32]. From the transport rate values, the nmol of Gln actually entered the internal space of proteoliposomes in 60 min can be derived (Table S1). The nmoles of Na$^+$ have been measured by the fluorometric assay in a parallel sample after 60 min (Table S2), as described in the section Spectrofluorometric assay. Then, nmoles of Gln and Na$^+$ have been compared to calculate the stoichiometry reported in the Results section. For the stoichiometry evaluation, proteoliposomes were prepared using 25 µg of recombinant hASCT2 in 50 mM NaCl buffer. Transport was started by adding 500 µM of external glutamine or [^{3}H]-glutamine in the presence of 50 mM Na-gluconate both for fluorometric and radiometric assay.

SDS/PAGE, and Western Blotting analysis

Protein amount was measured by densitometry of SDS/PAGE stained by Coomassie Blue, using the ChemiDoc imaging system equipped with Quantity One software (Bio-Rad Laboratories, Milano, Italy). The amount of incorporated protein was evaluated by western blot analysis using proteoliposome samples as prepared for transport assay. Immunoblotting analysis was performed using anti-His antibody 1 : 1000 (Merck Life Science), incubated 1 h in 3% BSA under shaking at room temperature and then revealed by chemiluminescence assay (Amersham™ ECLTM Prime Western Blotting Detection Reagent; Merck Life Science).

Data analysis

GRAFIT 5.0.13 Erithacus software (West Sussex, UK) was used to calculate kinetic parameters. Results were expressed as means ± SD. The statistical significance of experimental data was assessed by Student's test for $P < 0.05$ and $P < 0.01$, as specified in the figure legends.
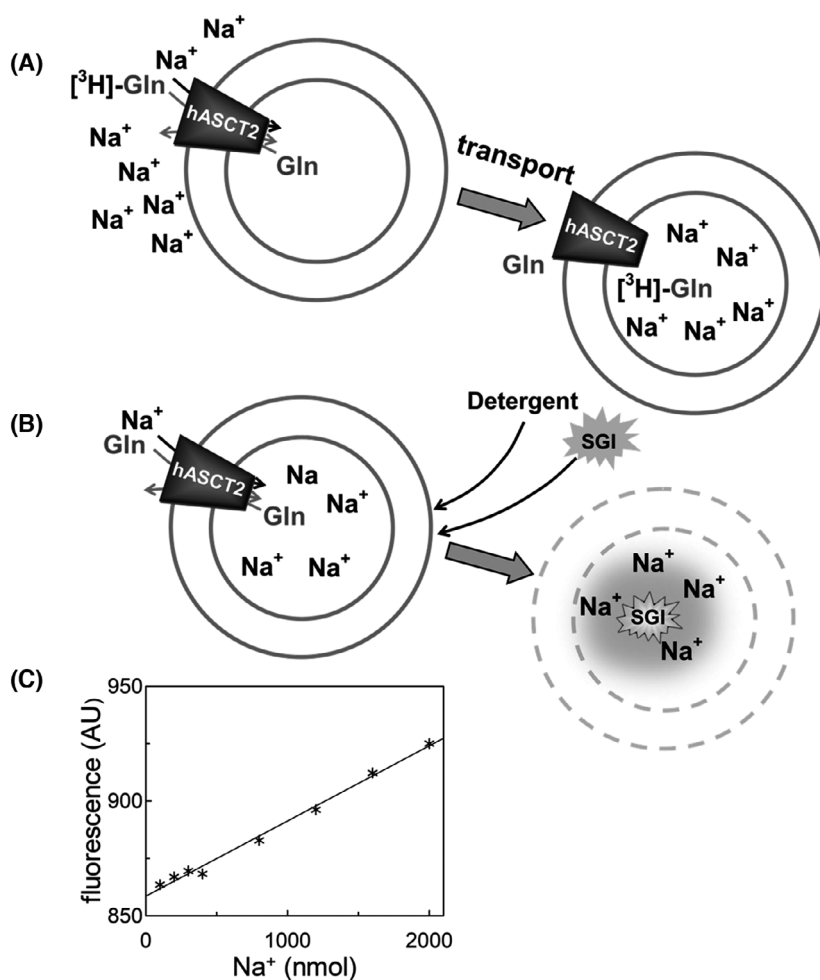
Fig. 1. Schematic representation of the three-substrate reaction measured in hASCT2-harbouring proteoliposome. In (A), internal unlabeled Gln is exchanged with external [^{3}H]-Gln and Na$^+$. In (B), schematic representation of fluorometric assay. After 60-min uptake, proteoliposome membrane was destabilized by adding detergent (0.25% C$_{12}$E$_8$) and 50 nM Sodium Green™ (SGI) as described in materials and methods. Released sodium was revealed by increased fluorescence signal of SGI. In (C), example of calibration line Fluorescence/nmol Na$^+$, performed at the end of each fluorometric measurement.

Results and Discussion

Effect of Na$^+$ on hASCT2 functionality

As stated in the introduction, the studies conducted so far on ASCT2, either murine or human isoforms showed the undoubted requirement of extracellular Na$^+$ for allowing the amino acid antiport across the cell membrane [1,2,13]. Much less is known about the role played by Na$^+$ in the intrinsic functionality and the transport reaction of the hASCT2. The availability of the recombinant hASCT2 reconstituted in proteoliposomes for transport assay, allowed us to shed light on these issues. Indeed, the proteoliposome model mimics the cell environment because the transporter is inserted into the artificial membrane with the same orientation it has in intact cells and with similar kinetics (Fig. 1A) [16]. Moreover, the proteoliposome tool is a single protein experimental model with no interferences from other transport/enzyme systems [33]. A further

advantage of using this experimental model is the possibility of specifically controlling the composition of the artificial membrane; indeed, it was previously shown that cholesterol included in the proteoliposome preparation increases the activity of hASCT2 by physical interaction with the protein [29]. To investigate the effect of Na$^+$ on the intrinsic functionality of hASCT2, the protein produced in *P. pastoris* was purified in the presence of increasing Na$^+$ concentrations in the buffers, following a protocol previously set up in our laboratory [8] (Fig. 2). Interestingly, the absence of Na$^+$ resulted in a complete loss of transport activity, whereas the addition of Na$^+$ to the purification buffers triggered an increase of the hASCT2 functionality in a concentration-dependent fashion (Fig. 2A). The effect of Na$^+$ was associated with the functionality of the protein; indeed, no variations on the yield of purified protein could be detected by changing Na$^+$ concentrations (Fig. 2B). A western blot analysis was conducted on proteoliposome samples obtained from the different

protein preparations of Fig. 2B to estimate the insertion of the protein in the vesicle membranes; interestingly, the insertion slightly enhanced with increasing the Na$^+$ concentration (Fig. 2C). This is further in line with a role for Na$^+$ in the activation, i.e. proper folding of the hASCT2, that improves the insertion of the protein into the membrane. To further assess that the positive effect of Na$^+$ was due to a prolonged protein-Na$^+$ interaction, the hASCT2 was added with sodium after the purification, just before the proteoliposome formation, i.e. during the detergent removal process described in the materials and methods section. As shown by Fig. 2D, the addition of 100 mM Na$^+$ after purification did not rescue the hASCT2 functionality. This last data gives a piece of additional information: the Na$^+$ contained in the protein buffer, that remains entrapped in the internal space of formed proteoliposomes, is not strictly required for the transport cycle. This conclusion correlates with the finding that the protein prepared in the presence of Na$^+$ and subjected to SEC eluted mostly at a molecular mass of about 150 KDa, corresponding to the trimeric active form of the protein (Fig. S4) [15]; whereas, the protein purified in the absence of Na$^+$ eluted entirely as high molecular mass aggregates (Fig. S5). To test the specificity of Na$^+$ on the hASCT2 functionality, the purification was performed in the presence of Na$^+$-gluconate, K$^+$-chloride or Li$^+$-acetate, in the place of NaCl. As shown in Fig. 3A, Na$^+$-gluconate and Na$^+$-chloride exerted similar effects in the maintenance of the protein in an active state, whereas the other cations, i.e. K$^+$ or Li$^+$ could not substitute for Na$^+$. Again, in favour of a 'structural' role of Na$^+$, no effect on the protein amount was observed upon the replacement of Na$^+$ (Fig. 3B) with the other cations. The same applies to the efficacy of reconstitution in proteoliposomes, which was only slightly impaired by Na$^+$ substitution (Fig. 3C). Furthermore, the effect of Na$^+$ on the transport activity of hASCT2 was independent on the presence of cholesterol included in the proteoliposome membrane (Fig. S6). Intriguingly, these results correlate with one of the key features of ASCT2 transport activity, observed since its first isolation in the 90's in both intact cells and proteoliposomes: the transport of the amino acids does not occur if Na$^+$ is substituted by Li$^+$ or K$^+$. Noteworthy, in the Cryo Electron Microscopy (CryoEM) structure(s) recently solved, no bound sodium ions have been described [15,34,35], even though sodium is always present in the buffers used for the CryoEM in good agreement with our purification methodology [8] and with the data on the requirement for Na$^+$ in the protein preparation here reported. These results correlate with a 'structural' role

of Na$^+$ probably in driving the proper protein folding and/or stability preventing aggregation, at least in the *in vitro* procedure. Then, Na$^+$ would act already upstream the transport reaction mediated by the reconstituted hASCT2.

Fluorometric measurement of Na$^+$ flux

To deeper dissect the role of Na$^+$ in the hASCT2 transport cycle, a method for detecting the intraliposomal accumulation of Na$^+$ has been pointed out using a fluorescent dye, the SGI (Fig. 1B). In agreement with the three-substrate transport reaction, a significant accumulation of Na$^+$ into proteoliposomes containing internal glutamine occurs only in the presence of both external Na$^+$ and glutamine (Fig. 4A). The intraliposomal Na$^+$ accumulation was much lower in the absence of externally added glutamine or in the absence of externally added Na$^+$ (Fig. 4A); in these conditions, the apparent accumulation of Na$^+$ was not statistically different from that measured with no additions (none, Fig. 4A). To evaluate hASCT2-mediated transport in a more physiological context, that is a hetero-exchange of neutral amino acids, glutamine was externally added together with Na$^+$ to proteoliposome containing internal serine (Na$^+$ − glutamine$_{ex}$/serine$_{in}$); in line with Na$^+$ − glutamine$_{ex}$/glutamine$_{in}$ data, a statistically significant accumulation of Na$^+$ was detected (Fig. 4B).

Kinetics of Na$^+$ transport

Using the same experimental setup, the accumulation of Na$^+$ as a function of external Na$^+$-gluconate concentration has been measured (Fig. 5A). As shown, the Na$^+$ accumulation increased with the external concentration and the data fitted a Michaelis–Menten equation; the measured Km was 15.0 ± 1.2 mM, i.e. nearly coincident with that obtained in a parallel radiometric assay measuring [3H]-glutamine transport as a function of the Na$^+$ concentration (Fig. 5B, Km 13.5 ± 2.3 mM and see also [8,16]). The coupled methodology of fluorometric and radiometric measurements was exploited to shed light on another open question around the hASCT2 transport cycle, that is the actual stoichiometry of Na$^+$ - amino acids co-transport. This experimental approach is similar to that employed to assess the stoichiometry of human SGLT1 [36]. Indeed, a comparison of the [3H]-glutamine uptake (123 ± 20 nmoles) with the fluorometric Na$^+$ accumulation (284 ± 93 nmoles) was performed and stoichiometry of roughly 1 Gln:2 Na$^+$ was calculated, as described in materials and methods section (Table 1 and Tables S1 and S2). Moreover,
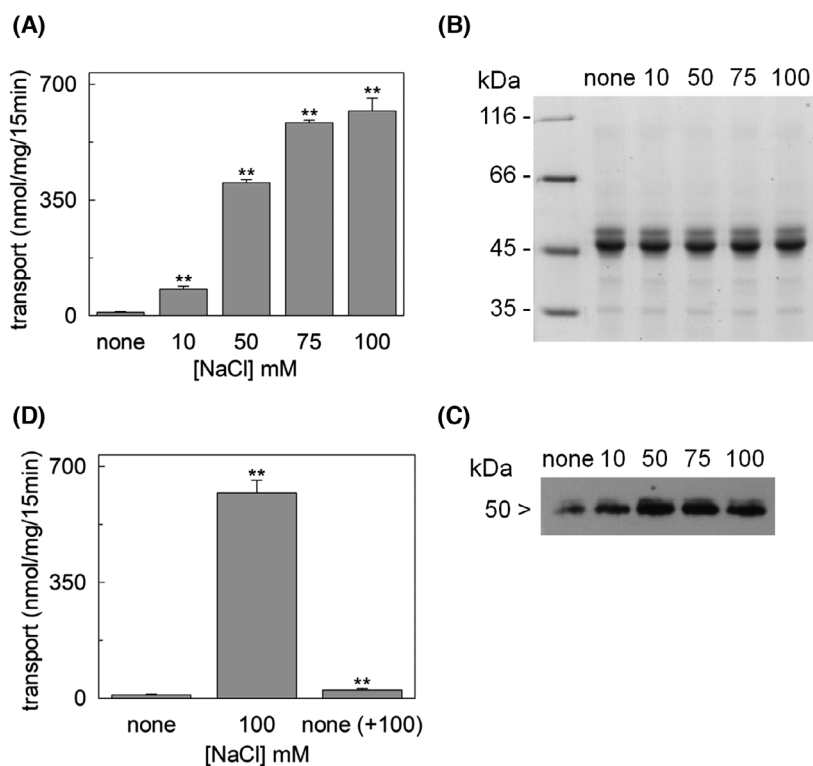
(A)

(B)

(D)

(C)

Fig. 2. Effect of Na$^+$ concentration on recombinant hASCT2 purification and functionality in proteoliposomes. Indicated concentrations of NaCl were added to the protein buffer during purification as described in materials and methods. In (A), proteoliposomes were prepared using recombinant hASCT2 purified in the presence of the indicated NaCl concentrations. The transport was started by adding 50 μM [^{3}H]-glutamine together with 50 mM Na-gluconate to proteoliposomes containing 10 mM internal glutamine. The transport was measured in 15 min according to the stop inhibitor method. Results are means ± SD from three independent experiments. Significantly different from the control sample (none) as estimated by Student's *t*-test **($P < 0.01$). In (B), Blue-Coomassie staining on SDS/PAGE analysis of recombinant hASCT2 purified in the presence of the indicated NaCl concentrations. Image is representative of three independent protein preparations. In (C), western blot analysis. Samples were obtained from proteoliposomes harbouring recombinant hASCT2 purified in the presence of the indicated NaCl concentrations. Image is representative of three independent experiments. In (D), proteoliposomes were prepared using recombinant hASCT2 purified in the absence of NaCl (none) or in the presence of 100 mM NaCl (100). The third sample is prepared using the protein purified in the absence of NaCl added with 100 mM NaCl before reconstitution (none + 100). The transport was started by adding 50 μM [^{3}H]-glutamine together with 50 mM Na-gluconate to proteoliposomes containing 10 mM internal glutamine. Results are means ± SD from three independent experiments. Significantly different from the control sample (none) as estimated by Student's *t*-test **($P < 0.01$).

moving from the Na$^+$ binding sites, which have been deeply characterized in ASCT1, and shown in Figs S2 and S3 [37], it was hypothesized that the Na$^+$ binding in hASCT2 may involve some charged amino acid residues whose interaction with the cation could be affected by changes in the pH of the transport assay. Then, the [^{3}H]-glutamine uptake, as a function of Na$^+$ concentration, was measured at pH 6.0 (Fig. 5C). Interestingly, and differently from the pH 7.0, the data fitted a Hill equation with a cooperativity index of 1.85 ± 0.32, as also shown by the slope of the derived graph (inset of Fig. 5C). Very importantly, the same results were obtained by directly measuring the Na$^+$ accumulation with the fluorometric assay (Fig. 5D and

inset of Fig 5D): by interpolating the data with a Hill equation, a cooperativity index of 1.74 ± 0.24 was derived, very similar to that obtained by the radiometric assay. The negative intercept at the y-axis indicates the number of Na$^+$ involved in the transport cycle or the number of Na$^+$ binding sites in the protein. These results correlated well with the transport/binding of two Na$^+$ by the hASCT2, in good agreement with the measured stoichiometry of 2Na$^+$: 1Gln (Table 1). The collected experimental results, in parallel to the *in silico* comparison with ASCT1 (Supplementary Figs 2 and 3), suggest an additional role for Na$^+$. Indeed, besides being directly transported by hASCT2, it is not trivial to hypothesize that the putative Na$^+$ binding

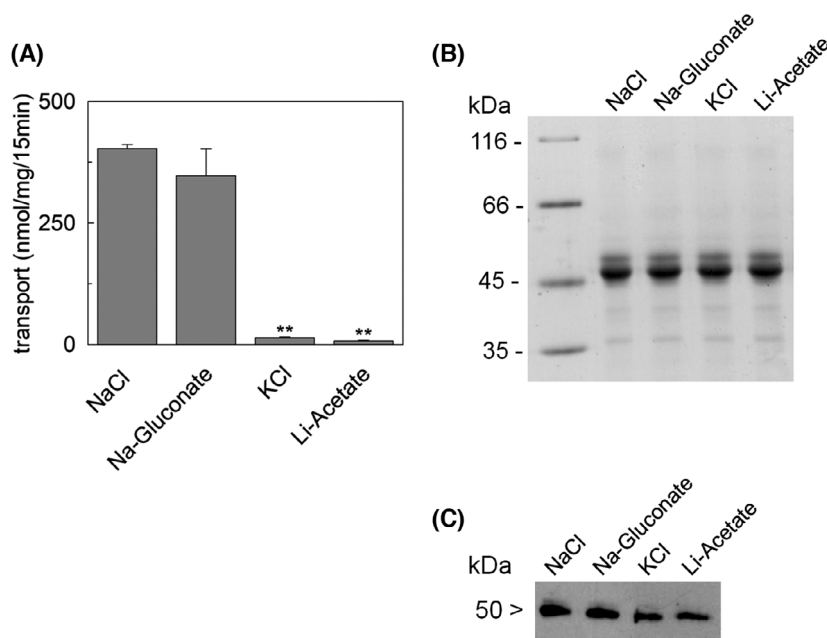**(A)**

(B)

(C)

Fig. 3. Effect of salt on hASCT2. Indicated salts were added to the protein purification buffer at 50 mM. In (A), proteoliposomes were prepared using recombinant hASCT2 purified in the presence of the indicated salts. The transport assay was started by adding 50 μM [^{3}H]-glutamine together with 50 mM Na-gluconate to proteoliposomes containing 10 mM internal glutamine. The transport was measured in 15 min according to the stop inhibitor method. Results are means ± SD from three independent experiments. Significantly different from the control sample (NaCl) as estimated by Student's *t*-test **($P < 0.01$). In (B), Blue-Coomassie staining on SDS/PAGE analysis of recombinant hASCT2 purified in the presence of the salts in the purification buffer. Image is representative of three independent preparations. In (C), western blot analysis. Samples were obtained from proteoliposomes harbouring recombinant hASCT2 purified in the presence of the indicated salts. Image is representative of three independent experiments.
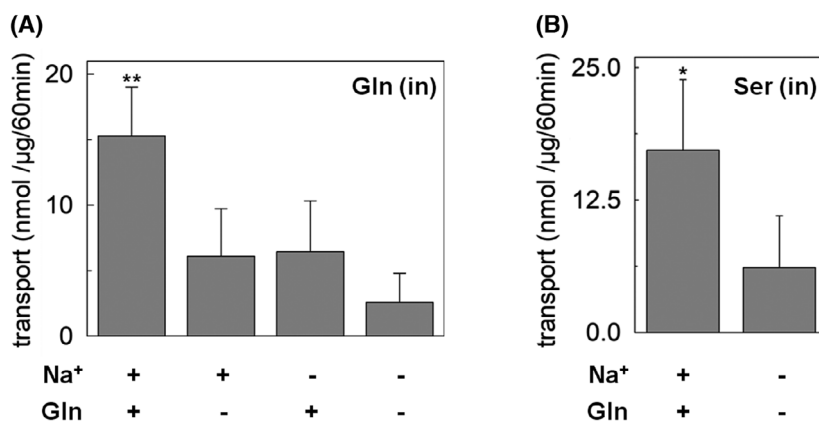
(A)

(B)

Fig. 4. Transport of Na$^+$ by hASCT2 reconstituted in proteoliposomes. In (A), the hASCT2 was purified in the presence of 50 mM NaCl, concentrated up to 1 μg·μL^{-1} and reconstituted in proteoliposomes containing 10 mM glutamine. The transport was started by adding 10 mM of glutamine (+) together (+) or not (-) with 50 mM Na-gluconate as indicated. As a control, assay without addition of external substrate was performed (−,−). The transport was measured in 60 min, according to the stop inhibitor method, and internal sodium concentration was measured by spectrofluorometric assay as described in materials and methods and in Fig 1B. The transport rate was expressed as nmol·μg^{-1}·60 min^{-1}. Results are means ± SD from six independent experiments. Significantly different from the control sample (without Gln and Na$^+$) as estimated by Student's *t*-test **($P < 0.01$). In (B), the same experiment was conducted in proteoliposomes containing 10 mM serine instead of glutamine. The transport was started by adding 10 mM of glutamine (+) together (+) with 50 mM Na-gluconate, as indicated. As a control, an assay without addition of external substrates was performed (-,-). Results are means ± SD from four independent experiments. Significantly different from the control sample (without Gln and Na$^+$) as estimated by Student's *t*-test *($P < 0.05$).
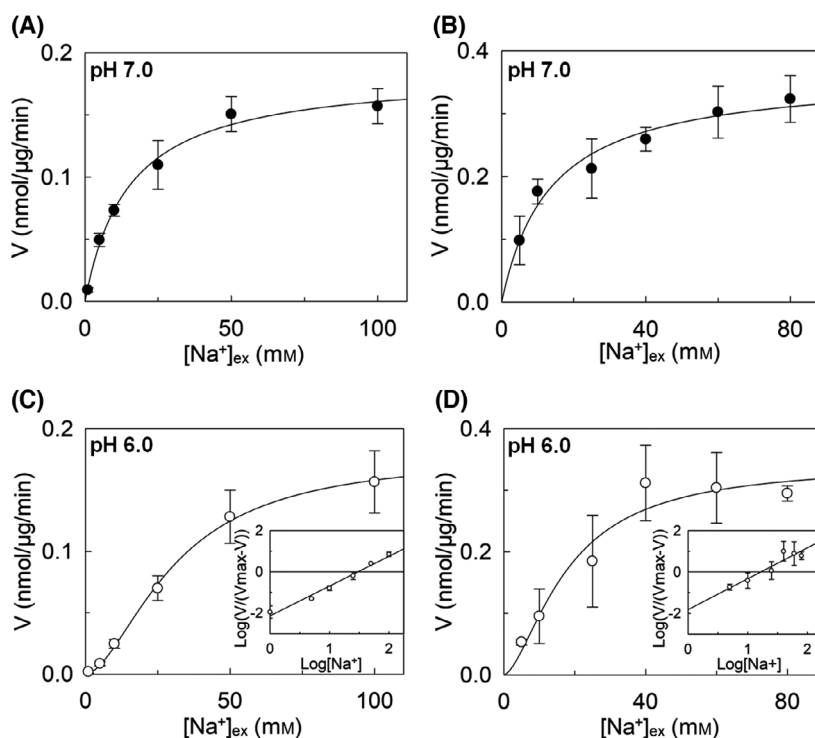
Fig. 5. Dependence of the transport rate of hASCT2 reconstituted in proteoliposomes on external Na$^+$ concentration. The hASCT2 was purified in the presence of 50 mM NaCl, concentrated up to 1 µg·µL^{-1} and reconstituted in proteoliposomes containing 10 mM glutamine. In (A) and (C), effect of pH on the kinetics of Na$^+$ transport measured with radiometric assay as described in materials and methods. Transport rate was measured by adding 50 µM [^{3}H]-glutamine to proteoliposomes in the presence of the indicated concentrations of Na-gluconate at pH 7.0 (A) or pH 6.0 (C). Data were plotted according to Michaelis–Menten equation (A) or Hill equation (C). Results are means ± S.D. from four independent experiments. In (B) and (D), kinetics of sodium transport measured by spectrofluorometric assay. The transport was started by adding 10 mM of glutamine to proteoliposomes in the presence of the indicated concentrations of Na$^+$-gluconate at pH 7.0 (B) or pH 6.0 (D). Transport was stopped in 60 min according to the stop inhibitor method and internal sodium concentration was measured by spectrofluorometric assay as described in materials and methods. Data were plotted according to Michaelis–Menten equation (B) or Hill equation (D). Results are means ± SD from four independent experiments. Insets in (C) and (D) represent the Hill linearization of data at pH 6.0.

sites on hASCT2, include both site(s) for transport and protein modulation and/or stability. Data on ASCT1, as well as on the bacterial orthologues of the SLC1 family, depicted a complex scenario in which, Na$^+$ interacts with three sites, namely Na1, Na2 and Na3. In particular, Na3 and Na1 are the highest affinity binding sites, being close in the structure and sharing one coordinating amino acid residue (Figs S2 and S3); whereas, Na2 is a low-affinity binding site most probably involved in conformational rearrangements, rather than in the Na$^+$ transport. Based on our data (Figs 2 and 3 and Fig. S4) we may hypothesize that the Na2 site could be involved in folding/stability preventing protein aggregation *in vitro*. Some of the described features are typical of other Na$^+$-dependent transporters, such as NSS, characterized by a LeuT fold for which different role(s) for Na$^+$ binding, transport and

regulation have been described in prokaryotic and eukaryotic proteins over the years [38–42].

Conclusions

The actual contribution of Na$^+$ to the function, stability and folding of Na$^+$-dependent transporters is an important issue that, over the years, revealed to be difficult to definitively address, mainly due to technical limitations. Indeed, even in the case of one of the most studied membrane proteins, i.e. LeuT, novel details on the Na$^+$ regulation and transport are continuously revealed [43]. Concerning eukaryotic proteins, studies are often delayed; indeed, to the best of our knowledge, the present study is the first one investigating the effect of Na$^+$ in both the intrinsic functionality and the transport cycle of

TABLE 1. Stoichiometry of the transport of sodium and glutamine by hASCT2. The hASCT2 was purified in the presence of 50 mM NaCl, concentrated up to 1 μg·μL^{-1} and reconstituted in proteoliposomes containing 10 mM glutamine. Transport was started by adding 500 μM glutamine or [^{3}H]-glutamine and 50 mM Na-gluconate. Data, expressed as nmol/60 min, was calculated as described in materials and methods. Results are means $\pm$ S.D. from four independent experiments. Significantly different as estimated by Student's *t*-test.

nmol Na$^+$/60 min	nmol Gln/60 min	*P*-value	Ratio Na$^+$/Gln
284 $\pm$ 93	123 $\pm$ 20	0.015	2.3

human ASCT2. Noteworthy, these achievements were reached using our model of hASCT2-harbouring proteoliposomes and setting up a fluorometric assay together with the more conventional radiometric approach. The results of this work show that Na$^+$ is crucial in the stability/folding of the recombinant hASCT2; it is important to stress that this effect has been described as relevant in the *in vitro* experimental procedures. However, it cannot be excluded that the cation could be also physiologically important in the folding process *in vivo*. Indeed, molecular mechanisms of the *in vivo* folding of membrane transporters are mostly unknown. Few exceptions are data on the trafficking and stability in the membrane of some proteins, including hASCT2 [9]. Altogether, the collected data show that the specificity for the 'structural' Na$^+$ overlaps the specificity for the 'functional' Na$^+$, shedding further light on the transport cycle of hASCT2. The main novelty of this work is that we could demonstrate, for the first time, that Na$^+$ is transported by hASCT2 from the external to the internal side of cell-mimicking vesicles with a calculated stoichiometry of 2Na$^+$:1 amino acid.

Acknowledgements

Author contributions

MS, TM and CI conceived, designed the experiments, and analysed the data. MS and TM performed the proteoliposome functional assays. LP and GP prepared the yeast constructs and optimized yeast cell growth. MS, TM and CI wrote the manuscript. CI supervised the entire work.

Data accessibility

The data that support the findings of this study are available from the corresponding author [cesare.indiveri@unical.it] upon reasonable request.

References

1 Kanai Y, Clemencon B, Simonin A, Leuenberger M, Lochner M, Weisstanner M and Hediger MA (2013) The SLC1 high-affinity glutamate and neutral amino acid transporter family. *Mol Aspects Med* **34**, 108–120.

2 Freidman N, Chen I, Wu Q, Briot C, Holst J, Font J, Vandenberg R and Ryan R (2020) Amino acid transporters and exchangers from the SLC1A family: structure, mechanism and roles in physiology and cancer. *Neurochem Res* **45**, 1268–1286.

3 Fuchs BC and Bode BP (2005) Amino acid transporters ASCT2 and LAT1 in cancer: partners in crime? *Semin Cancer Biol* **15**, 254–266.

4 Utsunomiya-Tate N, Endou H and Kanai Y (1996) Cloning and functional characterization of a system ASC-like Na+-dependent neutral amino acid transporter. *J Biol Chem* **271**, 14883–14890.

5 Torres-Zamorano V, Leibach FH and Ganapathy V (1998) Sodium-dependent homo- and hetero-exchange of neutral amino acids mediated by the amino acid transporter ATB degree. *Biochem Biophys Res Commun* **245**, 824–829.

6 Broer A, Brookes N, Ganapathy V, Dimmer KS, Wagner CA, Lang F and Broer S (1999) The astroglial ASCT2 amino acid transporter as a mediator of glutamine efflux. *J Neurochem* **73**, 2184–2194.

7 Oppedisano F, Pochini L, Galluccio M, Cavarelli M and Indiveri C (2004) Reconstitution into liposomes of the glutamine/amino acid transporter from renal cell plasma membrane: functional characterization, kinetics and activation by nucleotides. *Biochim Biophys Acta* **1667**, 122–131.

8 Pingitore P, Pochini L, Scalise M, Galluccio M, Hedfalk K and Indiveri C (2013) Large scale production of the active human ASCT2 (SLC1A5) transporter in *Pichia pastoris*–functional and kinetic asymmetry revealed in proteoliposomes. *Biochim Biophys Acta* **1828**, 2238–2246.

9 Console L, Scalise M, Tarmakova Z, Coe IR and Indiveri C (2015) N-linked glycosylation of human SLC1A5 (ASCT2) transporter is critical for trafficking to membrane. *Biochim Biophys Acta* **1853**, 1636–1645.

10 Gunnoo SB and Madder A (2016) Chemical protein modification through cysteine. *ChemBioChem* **17**, 529–553.

11 Scalise M, Console L, Galluccio M, Pochini L, Tonazzi A, Giangregorio N and Indiveri C (2019) Exploiting cysteine residues of SLC membrane transporters as targets for drugs. *SLAS Discov* **24**, 867–881.

12 Scalise M, Console L, Galluccio M, Pochini L and Indiveri C (2020) Chemical targeting of membrane transporters: insights into structure/function relationships. *ACS Omega* **5**, 2069–2080.

13 Scalise M, Pochini L, Console L, Pappacoda G, Pingitore P, Hedfalk K and Indiveri C (2018) Cys site-directed mutagenesis of the human SLC1A5 (ASCT2) transporter: structure/function relationships and crucial role of Cys467 for redox sensing and glutamine transport. *Int J Mol Sci* **19**, 648.

14 Bhutia YD and Ganapathy V (2016) Glutamine transporters in mammalian cells and their functions in physiology and cancer. *Biochim Biophys Acta* **1863**, 2531–2539.

15 Garaeva AA, Oostergetel GT, Gati C, Guskov A, Paulino C and Slotboom DJ (2018) Cryo-EM structure of the human neutral amino acid transporter ASCT2. *Nat Struct Mol Biol* **25**, 515–521.

16 Scalise M, Pochini L, Panni S, Pingitore P, Hedfalk K and Indiveri C (2014) Transport mechanism and regulatory properties of the human amino acid transporter ASCT2 (SLC1A5). *Amino Acids* **46**, 2463–2475.

17 Scalise M, Pochini L, Galluccio M, Console L and Indiveri C (2017) Glutamine transport and mitochondrial metabolism in cancer cell growth. *Front Oncol* **7**, 306.

18 Scalise M, Console L, Rovella F, Galluccio M, Pochini L and Indiveri C (2020) Membrane transporters for amino acids as players of cancer metabolic rewiring. *Cells* **9**, 2028.

19 Broer A, Rahimi F and Broer S (2016) Deletion of amino acid transporter ASCT2 (SLC1A5) reveals an essential role for transporters SNAT1 (SLC38A1) and SNAT2 (SLC38A2) to sustain glutaminolysis in cancer cells. *J Biol Chem* **291**, 13194–13205.

20 Broer S and Broer A (2017) Amino acid homeostasis and signalling in mammalian cells and organisms. *Biochem J* **474**, 1935–1963.

21 Scalise M, Mazza T, Pappacoda G, Pochini L, Cosco J, Rovella F and Indiveri C (2020) The human SLC1A5 neutral amino acid transporter catalyzes a pH-dependent glutamate/glutamine antiport, as well. *Front Cell Dev Biol* **8**, 603.

22 Broer A, Wagner C, Lang F and Broer S (2000) Neutral amino acid transporter ASCT2 displays substrate-induced Na+ exchange and a substrate-gated anion conductance. *Biochem J* **346** (Pt 3), 705–710.

23 Zander CB, Albers T and Grewer C (2013) Voltage-dependent processes in the electroneutral amino acid exchanger ASCT2. *J Gen Physiol* **141**, 659–672.

24 Oppedisano F, Pochini L, Galluccio M and Indiveri C (2007) The glutamine/amino acid transporter (ASCT2) reconstituted in liposomes: transport mechanism, regulation by ATP and characterization of the glutamine/glutamate antiport. *Biochim Biophys Acta* **1768**, 291–298.

25 Canul-Tec JC, Assal R, Cirri E, Legrand P, Brier S, Chamot-Rooke J and Reyes N (2017) Structure and allosteric inhibition of excitatory amino acid transporter 1. *Nature* **544**, 446–451.

26 Scalise M, Console L, Cosco J, Pochini L, Galluccio M and Indiveri C (2021) ASCT1 and ASCT2: brother and sister? *SLAS Discov* **26**, 1148–1163.

27 Oberg F, Sjohamn J, Conner MT, Bill RM and Hedfalk K (2011) Improving recombinant eukaryotic membrane protein yields in *Pichia pastoris*: the importance of codon optimization and clone selection. *Mol Membr Biol* **28**, 398–411.

28 Hanson MA, Cherezov V, Griffith MT, Roth CB, Jaakola VP, Chien EY, Velasquez J, Kuhn P and Stevens RC (2008) A specific cholesterol binding site is established by the 2.8 A structure of the human beta2-adrenergic receptor. *Structure* **16**, 897–905.

29 Scalise M, Pochini L, Cosco J, Aloe E, Mazza T, Console L, Esposito A and Indiveri C (2019) Interaction of cholesterol with the human SLC1A5 (ASCT2): insights into structure/function relationships. *Front Mol Biosci* **6**, 110.

30 Palmieri F and Klingenberg M (1979) Direct methods for measuring metabolite transport and distribution in mitochondria. *Methods Enzymol* **56**, 279–301.

31 Solenov EI (2008) Cell volume and sodium content in rat kidney collecting duct principal cells during hypotonic shock. *J Biophys* **2008**, 420963.

32 Palmieri F, Indiveri C, Bisaccia F and Iacobazzi V (1995) Mitochondrial metabolite carrier proteins: purification, reconstitution, and transport studies. *Methods Enzymol* **260**, 349–369.

33 Scalise M, Pochini L, Giangregorio N, Tonazzi A and Indiveri C (2013) Proteoliposomes as tool for assaying membrane transporter functions and interactions with xenobiotics. *Pharmaceutics* **5**, 472–497.

34 Yu X, Plotnikova O, Bonin PD, Subashi TA, McLellan TJ, Dumlao D, Che Y, Dong YY, Carpenter EP, West GM *et al.* (2019) Cryo-EM structures of the human glutamine transporter SLC1A5 (ASCT2) in the outward-facing conformation. *Elife* **8**, e48120.

35 Garaeva AA, Guskov A, Slotboom DJ and Paulino C (2019) A one-gate elevator mechanism for the human neutral amino acid transporter ASCT2. *Nat Commun* **10**, 3427.

36 Jiang X, Loo DD, Hirayama BA and Wright EM (2012) The importance of being aromatic: pi interactions in sodium symporters. *Biochemistry* **51**, 9480–9487.

37 Scopelliti AJ, Heinzelmann G, Kuyucak S, Ryan RM and Vandenberg RJ (2014) Na+ interactions with the neutral amino acid transporter ASCT1. *J Biol Chem* **289**, 17468–17479.

38 Yamashita A, Singh SK, Kawate T, Jin Y and Gouaux
    E (2005) Crystal structure of a bacterial homologue of
    Na+/Cl–dependent neurotransmitter transporters.
    Nature **437**, 215–223.

39 Khafizov K, Perez C, Koshy C, Quick M, Fendler K,
    Ziegler C and Forrest LR (2012) Investigation of the
    sodium-binding sites in the sodium-coupled betaine
    transporter BetP. *Proc Natl Acad Sci USA* **109**, E3035–
    E3044.

40 Watanabe A, Choe S, Chaptal V, Rosenberg JM,
    Wright EM, Grabe M and Abramson J (2010) The
    mechanism of sodium and substrate release from the
    binding pocket of vSGLT. *Nature* **468**, 988–991.

41 Hummel CS, Lu C, Loo DD, Hirayama BA, Voss AA
    and Wright EM (2011) Glucose transport by human
    renal Na+/D-glucose cotransporters SGLT1 and
    SGLT2. *Am J Physiol Cell Physiol* **300**, C14–21.

42 Wahlgren WY, Dunevall E, North RA, Paz A, Scalise
    M, Bisignano P, Bengtsson-Palme J, Goyal P, Claesson
    E, Caing-Carlsson R *et al.* (2018) Substrate-bound
    outward-open structure of a Na(+)-coupled sialic acid
    symporter reveals a new Na(+) site. *Nat Commun* **9**, 1753.

43 Fan J, Xiao Y, Quick M, Yang Y, Sun Z, Javitch JA
    and Zhou X (2021) Crystal structures of LeuT reveal
    conformational dynamics in the outward-facing states.
    J Biol Chem **296**, 100609.

Supporting information

Additional supporting information may be found
online in the Supporting Information section at the end
of the article.

Fig. S1. Alignment of amino acid sequences of human,
mouse and rat ASCT2.

Fig. S2. Alignment of hASCT1 and hASCT2 amino
acid sequences. Alignment was performed using
Clustal Omega software. Identities are indicated by
asterisks and conservative or highly conservative sub-
stitutions are indicated by dots or colons, respectively.
Residues corresponding to the three hASCT1 binding
sites, conserved in hASCT2, are highlighted with dif-
ferent colours: yellow for sodium binding site 1 (Na1),
cyan for sodium binding site 2 (Na2), red for sodium
binding site 3 (Na3) and orange for both sodium bind-
ing site 1 and 3 (Na1 & Na3).

Fig. S3. Structure of hASCT2 with putative sodium
binding sites. In A), the cryo-EM structure of hASCT2
in an inward-occluded conformation (PDB ID:
6GCT). The structure is represented as a monomer in
dark grey and the three sodium binding sites are high-
lighted with different colours: yellow for sodium bind-
ing site 1 (Na1), cyan for sodium binding site 2 (Na2)
and red for sodium binding site 3 (Na3). Structure is
represented using PyMOL v2.4.1 software. In B),
zoomed box with residues belonging to the sodium
binding sites 1 (Na1) in yellow and sodium binding
sites 2 (Na2) in cyan. In C), zoomed box with residues
belonging to the sodium binding site 3 (Na3) in red.

Fig. S4. SDS/PAGE analysis of hASCT2 SEC in the
presence of Na+.

Fig. S5. SDS/PAGE analysis of hASCT2 SEC without
Na+.

Fig. S6. Effect of cholesterol and external Na+ on
hASCT2 activity in proteoliposomes.

Table S1. Calculations of the glutamine uptake in
60 min from experimental data as described in Materi-
als and methods section "Stoichiometry evaluation".

Table S2. Data of Na+ uptake calculated as described
in Materials and methods "spectroflurometric assay"
section.